CHEMICAL ENGINEERING TRANSACTIONS
VOL. 65, 2018
A publication of AIDIC
The Italian Association of Chemical Engineering
Online at www.aidic.it/cet
Guest Editors: Eliseo Ranzi, Mario Costa

ISBN 978-88-95608- 62-4; **ISSN** 2283-9216

Laser-Based Spectroscopy Diagnosis and Detailed Numerical Models to Gain Understanding on the Slow Pyrolysis Behavior of Thermally Thick Wood Particles

Hernán Almuina-Villar[a], Andrés Anca-Couce[b], Norbert Lang[c], Jürgen Röpcke[c], Frank Behrendt[a], Alba Dieguez-Alonso*[,a]

[a]Technische Universität Berlin, Institute of Energy Engineering, Fasanenstr. 89 10623 Berlin, Germany
[b]Institute of Thermal Engineering, Graz University of Technology, Inffeldgasse 25b, 8010 Graz, Austria
[c]Leibniz Institute for Plasma Science and Technology, Felix-Hausdorff-Str. 2 17489 Greifswald, Germany
alba.dieguezalonso@tu-berlin.de

The slow pyrolysis behaviour of thermally thick wood particles is investigated at 5, 10 and 20 ºC/min, combining an advanced single-particle experimental approach with a detailed numerical model. Infrared laser absorption spectroscopy (IRLAS) and laser-induced fluorescence spectroscopy (LIF) are used to characterize on-line and in-situ the evolution of the following volatile products in the close vicinity of the pyrolysing particle: CO_2, CO, CH_4, H_2O, CH_2O and fluorescence-emitting species with excitation wavelengths of 266 and 355 nm, such as polycyclic aromatic hydrocarbons (PAH). The numerical particle model is coupled with a detailed pyrolysis kinetic scheme, being able to predict with good accuracy mass loss, temperature evolution and online release of species such as H_2O and CO. Model predictions are in some cases even better than for the medium heating rate conditions for which the model was initially tested, showing its wide applicability. Furthermore, the model can be improved including PAH release, for which experimental data is presented, and the delayed release of CH_4, which is not correctly described by the model at low heating rates.

1. Introduction

Pyrolysis is a key stage in any thermochemical conversion of biomass (White et al., 2011), influencing aspects of the process, such as technology design and scale-up or emissions (Nussbaumer, 2010). Despite its relevance, and due to its high complexity, enhanced by the interaction of chemical pathways and physical transport phenomena, the exact pyrolysis mechanism is still unknown (White et al., 2011).
In fixed-bed thermochemical conversion processes (gasification, combustion, slow pyrolysis), particle sizes in the centimeter scale are typically used (Miller et al., 1997; Bennadji et al., 2014), which can have a strong influence on the pyrolysis mechanism (Bennadji et al., 2014; Corbetta et al., 2014; Lang et al., 2017) due to the presence of intra-particle secondary reactions, along with intra-particle temperature gradients.
The current understanding of pyrolysis reaction mechanisms has been recently reviewed by Anca-Couce (2016), pointing out that the kinetic schemes based on the one developed by Ranzi et al. (2008), treating biomass as five components (cellulose, hemicellulose and three types of lignin), are the most detailed.
Ranzi´s scheme has been applied in several single-particle models, reproducing the pyrolysis of thermally thick wood particles. Corbetta et al. (2014) developed a single-particle model adapting Ranzi´s scheme and including homogeneous secondary reactions of the pyrolysis volatiles (Ranzi et al., 2014), as well as the transport model developed by Park et al. (2010). Although the model (Corbetta et al., 2014) showed promising results for mass loss, temperature evolution and characterization of the released species, as highlighted by the authors, its further improvement would require the inclusion of heterogeneous secondary reactions. This adaptation of Ranzi's scheme (Corbetta et al., 2014) was also used by Bennadji et al. (2014). It was pointed out that future improvement of the kinetic scheme should include intra-particle tar reactions, as well as a reevaluation of kinetic parameters for the early evolution of gas species (Bennadji et al., 2014). Anca-Couce et al. (2014) adapted Ranzi´s scheme to include the presence of secondary char-forming reactions, relevant in

pyrolysis of thermally thick particles, as previously mentioned. In a recent study, Anca-Couce et al. (2017a) compared detailed experimental results at particle level with the results of a particle model using three different versions of Ranzi´s scheme: (1) the adaptation of Ranzi´s scheme by Anca-Couce et al. (2014) including secondary charring reactions (Version 1); (2) the adaptation of Ranzi´s scheme by Corbetta et al. (2014), including secondary charring reactions (Version 2); and (3) an improvement of Version 2, mainly regarding char yield and composition, as well as the release of light hydrocarbons, based on experimental results (Version 3). Version 3 (called in the following RAC V3) showed the best results, which included temperature in the centre and surface of the particle, mass loss and dynamic evolution of CO, H_2O, CO_2, CH_4, other light hydrocarbons and light condensable species (formaldehyde, acetic acid, methanol, ethanol, acetaldehyde and acetic acid), characterized on-line and off-situ with Fourier-transform infrared absorption (FTIR), and levoglucosan, measured off-line by gas chromatography – mass spectrometry (GC-MS). Despite the achieved improvements, the authors highlighted the need to include the influence of inorganic species on the pyrolysis mechanism, the description of secondary charring reactions with Arrhenius equations (instead of fitted parameters) and the formation of PAH (polyaromatic hydrocarbons), BTX (benzene toluene xylene) and soot, accompanied by a more detailed characterization of the volatile products and validation under different conditions.

Quantification of volatiles in single-particle pyrolysis experiments has been done predominantly in an ex-situ manner, either online or offline, usually applying FTIR and chromatography techniques (deJong et al., 2003, Anca-Couce et al., 2017a). However, in order to correctly characterize the volatiles produced during pyrolysis, in-situ techniques should be preferred, with the objective of avoiding possible further reactions of the targeted species. Zobel and Anca-Couce (2013) applied laser-induced fluorescence (LIF) spectroscopy to detect PAHs formed during pyrolysis of thermally thick wood particles. Lang et al. (2017) combined two laser-based spectroscopy techniques (IRLAS - infrared laser absorption spectroscopy - and LIF) to analyse the volatiles composition in the close vicinity of a pyrolysing particle.

The objective of the present study is to compare the experimental characterization (particle mass and temperature evolution; release of volatile species) of a single pyrolysing wood particle with the results obtained from the particle model developed by Anca-Couce et al. (2017a), using the adaptation of Ranzi´s pyrolysis kinetic scheme (RAC V3) carried out by Anca-Couce et al. (2017a). The particle model was adapted in the present study to meet the conditions used in the experiments. For the experimental characterization of the volatiles release, the innovative approach, based on the combination of two laser-based spectroscopy tecniques (LIF and IRLAS), previously introduced, was used. These experiments were performed with beech wood spheres, with a diameter of 25 mm, at three heating rates: 5, 10 and 20 °C/min. The experimental results have been published in Lang et al. (2017). Moreover, the experimental and modelled volatiles evolution reported by Anca-Couce et al. (2017a) are also used in the present study for comparison. In Anca-Couce et al. (2017a), medium heating rates (> 150 °C/min) and smaller particles (spruce cylindrical pellets with a diameter of 8 mm and a length of 19 mm) were employed. This novel comparison between numerical and experimental results under different conditions, including different experimental setups, will bring new insights into the pyrolysis reaction mechanism and the influence of secondary charring reactions.

2. Experimental and model description

Table 1: Raw materials properties

	Beech	Spruce
Volatiles (% wt., db)	85.60 ± 0.20	-
Ash (%wt., db)	0.41 ± 0.01	0.40
Fixed. Carbon (%wt., db)	13.98 ± 0.20	-
Moisture (% wt.)	-	8
C(% wt., db)	48.35 ± 0.14	50.15
N(% wt., db)	0.09 ± 0.00	-
H(% wt., db)	6.87 ± 0.04	6.23
S(% wt., db)	0.06 ± 0.02	-
O(% wt., db)	44.65 ± 0.15	-
Apparent density, g/cm^3	0.708 ± 0.034	1.120

The experimental setup used to perform the single particle pyrolysis experiments has been presented elsewhere (Lang et al., 2017). Dried beech spheres (Ø=25 mm; mass around 5.5 g) were used. Characterization of this material is given in Table 1. Three heating rates, 5, 10 and 20 °C/min were applied until a final temperature of 600 ºC. Moreover, the experimental results published by Anca-Couce et al. (2017a) were employed in the present study for comparison purposes. These experimental results were obtained from pyrolysis of spruce pellets (Ø=25 mm, L=9 mm; mass around 1.5 g), conducted at higher heating rates (> 150 °C/min) until a final temperature of 550 ºC. The particle model used in the present study has been developed by Anca-Couce et al. (2017a). This model uses the adaptation (RAC V3) of Ranzi´s kinetic scheme developed by Anca-Couce et al. (2017a), based on an earlier adaptation of Ranzi´s kinetic scheme developed by Corbetta et al. (2014).

*Table 2: Single-particle model parameters changed in the present study with respect to Anca-Couce et al. (2017a). *Taken from (Gauthier et al., 2013). **The temperatures measured in the particle-level reactor were taken as boundary conditions. For convective heat transfer, the temperature measured in the atmosphere, in the close vicinity of the pyrolysing particle, was used. For radiation, an average of the temperatures measured in the particle-level reactor walls (externally heated) was used. ***Temperature-dependent gas velocity.*

Properties	Present study	Anca-Couce et al., 2017a
Porosity	0.53	0.2
*Cellulose [%]	42	44
*Hemicell. [%]	31.5	26
*Lignin-C [%]	13	17.5
*Lignin-H [%]	1.6	9.5
*Lignin-O [%]	11.9	3
X_{CEL}	0.2	0.05
X_{HCE}	0.2	0.1
X_{LIG}	0.3	0.15
$X_{G\{\}}$	0.4	0.2
**$T_{heating}$ [°C]	T_{amb} – 600°C	550
***Gas vel. [m/s]	0.03 – 0.10	0.35
Geometry	Sphere (Ø=25 mm)	Cylinder (Ø=8 mm; L=19 mm)

In the RAC V3 scheme, secondary charring reactions are included, as well as further adjustments (volatiles composition and stoichiometric factors) in Corbetta's scheme, based on comparison with experimental data from Anca-Couce et al. (2017a). The introduction of secondary charring reactions was done in the form of fitting parameters, X_{CEL}, X_{HCE}, X_{LIG} and $X_{G\{\}}$, introduced in Table 2 (Anca-Couce et al., 2017a; Anca-Couce et al., 2017b). They represent the extent of these reactions in cellulose, hemicellulose and lignin pyrolysis, as well as secondary reactions in the char formed at lower temperatures ($X_{G\{\}}$). Biomass is treated as five independent pseudo-components: cellulose, hemicellulose and three types of lignin (depending on the proportion of C, H and O).

To meet the experimental conditions pertinent to the experimental results presented in this study (Lang et al., 2017), several model parameters were modified with respect to the ones presented by Anca-Couce et al. (2017a), shown in Table 2. No homogeneous tar cracking reactions in the reactor were considered due to the low temperatures. Other model parameters remained unchanged.

3. Results and discussion

In Figure 1, the comparison between experimental and numerical results is presented for the time-dependent evolution of the solid mass fraction and the temperature in both center and surface of the particle. The experimental temperature evolution at 10 °C/min and the experimental mass loss evolution at 5, 10 and 20 °C/min have been already published in a recent work of this group (Lang et al., 2017). It is important to clarify that while the model gives the temperature on the particle surface, experimentally this was measured in the close vicinity of the particle, i.e., a few mm from the particle surface. This could explain the differences between model and experiments at low temperatures. The experimental mass loss evolutions and solid yields (Figure 1, top) were well predicted by the model, specially at the lowest heating rates, 5 and 10 °C/min. With respect to the temperature in the center of the particle, the model was able to reproduce the exothermicity present in all cases, identified when the temperature in the center of the particle exceeded the temperature on the surface of the particle. This exothermicity was also stronger with higher heating rates and, at each heating rate, two exothermic regimes were identified. These were associated to hemicellulose decomposition and to the overlapping of primary cellulose decomposition and lignin, and linked with heterogeneous secondary reactions of the primary volatiles (Lang et al., 2017).

Table 3: Yields of the main characterized volatile species. The experimental results from the "present study" have been published in a recent work of this group (Lang et al., 2017).

Yields (%)	Present study		Anca-Couce (2017a)	
	Experimental	Model	Experimental	Model
H_2O	16.4	14.2	18.0	16.4
CO	6.1	6.3	4.8	6.2
CO_2	2.9	14.4	11.6	11.4
CH_4	1.6	1.3	1.5	1.4

In the detailed kinetic scheme coupled to the particle model, used in the present study and developed by Anca-Couce et al. (Anca-Couce et al., 2017a, and Anca-Couce et al., 2017b), the presence and extent of exothermic heterogeneous charring reactions were determined by a factor "X" for each pseudo-component. This was the only factor "fitted" in the present model, to get a good agreement between model and experiments, regarding final char yield and temperature evolution.

The "X" factors for all pseudo-components increased with respect to the values used by Anca-Couce et al (2017a), and they were very similar to the values suggested for high charring conditions in Anca-Couce et al (2017b). This indicates that the extent of secondary charring reactions during pyrolysis of a beech particle (in Lang et al., 2017) was higher than for pyrolysis of a spruce particle (in Anca-Couce et al., 2017a), where the heating rates were higher (> 150 °C/min) and the particle size smaller, as presented in Section 2.

In Figure 2, a comparison between numerical and experimental results for release of H_2O (a), CO_2 (b), CO (c), CH_4 (d) and CH_2O (e) during pyrolysis of beech at 5 °C/min is presented. The concentration of these species was determined with IRLAS in the close vicinity of the particle, as introduced in Section 2. Both numerical and experimental results from the present work are also compared with the numerical and experimental results from Anca-Couce et al. (2017a). The differences in heating rate and initial mass explain the difference in the release values, expressed in g/s, between the two sets of results. The yields of the measured volatile species are also compared in Table 3.

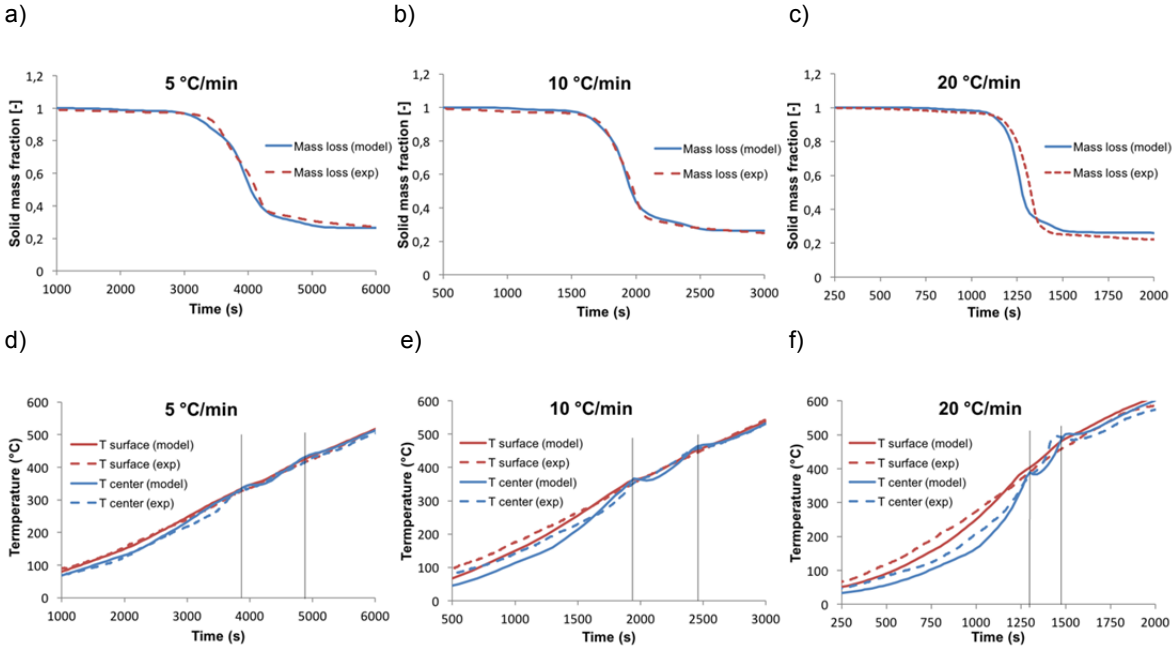

Figure 1: Comparison of mass loss (top) and temperature evolution (bottom) between experimental (dashed lines) and numerical (solid lines) results for pyrolysis of a beech particle at 5, 10 and 20 °C/min. For temperature comparison, red lines represent the surface temperature and blue lines the temperature in the centre of the particle. The experimental results for mass loss and temperature evolution at 10 °C/min have been published in a study of this group (Lang et al., 2017). Vertical lines distinguish the exothermic regions.

For H_2O and CO there is remarkable good agreement between numerical and experimental results (Figure 2 and Table 3) in the present study, even better than those for A-C (Anca-Couce et al., 2017a). This supports the applicability of the model for a wide variety of experimental conditions. For CO_2 and CH_4 the fitting was not as good. One of the reasons is the technical limitations of the IRLAS technique to measure CO_2, due to the influence of temperature in these measurements (Lang et al., 2017). This could lead to a lower measured CO_2 yield and will be addressed in future work of this group. For CH_4, however, these limitations were in principle not present. CH_4 yields were predicted with a good accuracy (Table 3), but CH_4 was released mainly at the end of the experiment, i.e. at high conversions, which was not completely captured by the model, specially for the results of this study at low heating rates. The pyrolysis reaction scheme has been already adapted in Anca-Couce et al. (2017a) to account, to some extent, for this delayed release at medium heating rates (A-C in Figure 2, d). The novel results at low heating rates in this study show, however, that further modifications are still needed in order to correctly predict the delayed release of light hydrocarbons. The CH_4 evolution is presented normalized for a better comparison between model and experiments, so that CH_4 release, especially at low heating rates, is clearly seen, as it takes place mainly at the end of the experiment, in a period with a small variation in total conversion, and slowly, achieving low values in g/s.

In Figure 2, e) the normalized values of formaldehyde (the time-dependent evolution was measured in this study, but not the absolute concentration) are also compared. It is possible to see that the behaviour was different in both cases. In the present study, there were two regions of emission, one at low conversion, coincident with hemicellulose decomposition and a second one at higher conversion, coincident with the emission of CO and other species, i.e., with the main decomposition of cellulose. The model can qualitative predict these two regions observed in the experimental results at a low heating rate. In the case of A-C´s results, only one region was present, probably due to the merging of the two aforementiond regions at higher heating rates. In Figure 2, f) the qualitative evolution of species that can emit fluorescence when excited at 266 and 355 nm is compared with the model derived evolution of light condensables (LC) (carbonyls and

alcohols, including formaldehyde and other species) and heavy condensables (HC) (5-hydroxymetylfurfural, phenolics and sugars). The fluorescending species at these excitation wavelengths should be mainly PAHs (Lang et al., 2017, Dieguez-Alonso et al., 2015). It is then observed that the emission of PAHs, coming from secondary reactions, was delayed with respect to the emission of the pyrolysis condensable volatiles. This data can be employed to further improve pyrolysis models including PAH release.

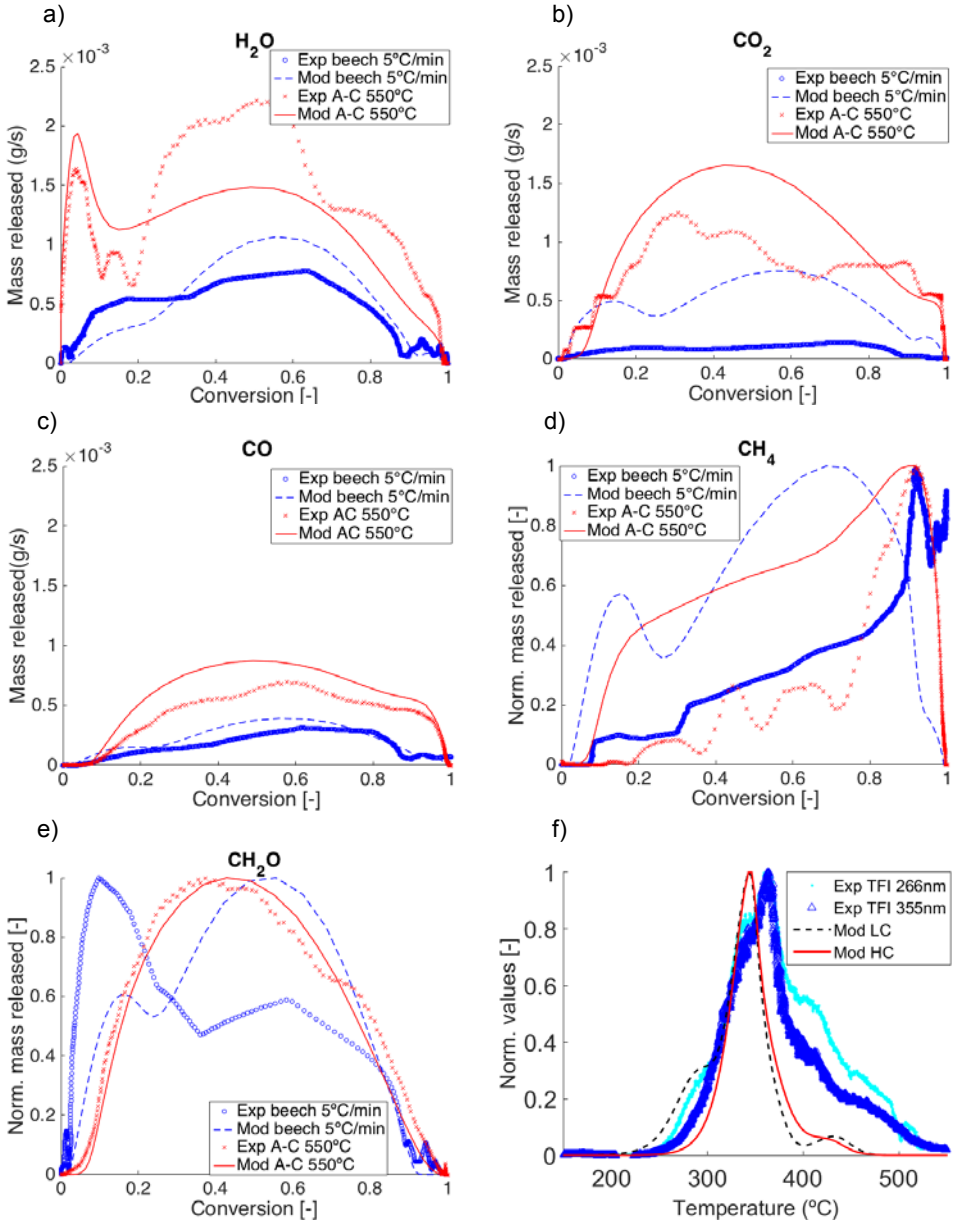

Figure 2: Comparison for a) H_2O, b) CO_2, c) CO, d) CH_4 (normalized), e) CH_2O (normalized) production between numerical and experimental results. The experimental results (blue circles) of the present study were published in Lang et al. (2017), except for CH_2O. In red, the results from Anca-Couce et al. (2017a) are shown. f) Comparison between the evolution of fluorescending species determined with 355 and 266 excitation wavelengths and the numerical results for light condensables (LC) and heavy condensables (HC) from the present study.

4. Conclusions

A detailed experimental characterization of the slow pyrolytic behaviour of a thermally thick wood particle (beech) is compared with the results of a particle model, including a detailed pyrolysis scheme, with 22 volatile species, and accounting for the influence of secondary charring reactions. The experimental characterization was performed with an innovative experimental approach, combining two spectroscopy techniques (IRLAS and LIF). The model was able to properly predict mass loss, temperature in the center and surface of the

particle and the evolution of volatile species, such as H_2O and CO, in conditions enhancing secondary charring reactions. The obtained results were in some cases even better than for the medium heating rate conditions for which the model was initially tested, with a lower extent of secondary charring reactions. This shows the wide applicability of the model and the suitability of volatiles characterization with sensitive on-line and in-situ techniques. The results also show that although the total yield of CH_4 was well predicted, the delayed CH_4 release was not correctly described by the model at low heating rates. Experimental data for future model improvements including PAHs release were also provided.

Acknowledgments

The experimental work relative to slow pyrolysis of beech particles with the application of two different laser-based spectroscopy techniques for volatiles characterization was funded by the German Research Foundation (DFG) within the framework of the projects FKZ: BE 1473/5-1 and RO 2202/8-1. The authors thank the German Research Foundation for its support.

References

Anca-Couce A., Mehrabian R., Scharler R., Obernberger I., 2014, Kinetic scheme of biomass pyrolysis considering secondary charring reactions, *Energy Convers Manage*, 87, 687–96.

Anca-Couce A., 2016, 'Reaction mechanisms and multi-scale modelling of lignocellulosic biomass pyrolysis', *Prog. Energy Combust. Sci*. 53, 41–79.

Anca-Couce A., Sommersacher P., Scharler R., 2017a, Online experiments and modelling with a detailed reaction scheme of single particle biomass pyrolysis*, J. Anal. Appl. Pyrolysis*, 127, 411-425.

Anca-Couce A., Scharler R., 2017b, Modelling heat of reaction in biomass pyrolysis with detailed reaction schemes, *Fuel*, 206, 572–579.

Bennadji H., Smith K., Serapiglia M.J., Fisher E.M., 2014, Effect of particle size on low temperature pyrolysis of woody biomass, *Energy Fuels,* 28 (12), 7527–7537.

Corbetta M., Frassoldati A., Bennadji H., Smith K., Serapiglia M.J., Gauthier G., Melkior T., Ranzi E., Fisher E.M., 2014, Pyrolysis of centimeter-scale woody biomass particles: kinetic modeling and experimental validation, *Energy Fuels*, 28 (6), 3884–3898.

Dieguez-Alonso A., Anca-Couce A., Zobel N., Behrendt F., 2015, Understanding the primary and secondary slow pyrolysis mechanisms of holocellulose, lignin and wood with laser-induced fluorescence, *Fuel*,153, 102–109.

Gauthier G., Melkior T., Salvador S., Corbetta M., Frassoldati A., Pierucci S., Ranzi E., Bennadji H., Fisher E.M., 2013, Pyrolysis of thick biomass particles: Experimental and kinetic modelling, *Chemical Engineering Transactions*, 32, 601-606.

de Jong W., Pirone A., Wojtowicz M.A., 2003, Pyrolysis of Miscanthus Giganteus and wood pellets: TG-FTIR analysis and reaction kinetics, *Fuel*, 82, 1139.

Lang N., Rupp C., Almuina-Villar H., Dieguez-Alonso A., Behrendt F., Röpcke J., 2017, Pyrolysis behavior of thermally thick wood particles: Time-resolved characterization with laser based in-situ diagnostics, *Fuel*, 210, 371-379.

Miller R.S., Bellan J., 1997, A generalized biomass pyrolysis model based on superimposed cellulose, hemicellulose and lignin kinetics, *Combust. Sci. Technol*., 126, 97−137.

Nussbaumer T., 2010, Overview on technologies for biomass combustion and emission levels of particulate matter, prepared for Swiss Federal O□ce for the Environment (FOEN) as a contribution to the Expert Group on Techno-Economic Issues (EGTEI) under the Convention on Long-Range Transboundary Air Pollution (CLRTAP). Tech. rep., Verenum. Ingenieurbüro für Verfahrens-, Energie- und Umwelttechnik.

Park W.C., Atreya A., Baum H.R., 2010, Experimental and theoretical investigation of heat and mass transfer processes during wood pyrolysis, *Combust. Flame,* 157(3), 481–94.

Ranzi E., Cuoci A., Faravelli T., Frassoldati A., Migliavacca G., Pierucci S., Sommariva S., 2008, Chemical kinetics of biomass pyrolysis, *Energy Fuels*, 22 (6), 4292–4300.

Ranzi E., Corbetta M., Manenti F., Pierucci S., 2014, Kinetic modeling of the thermal degradation and combustion of biomass, *Chem. Eng. Sci.*, 110, 2−12.

White J.E., Catallo W.J., Legendre B.L., 2011, Biomass pyrolysis kinetics: a comparative critical review with relevant agricultural residue case studies, *J. Anal. Appl. Pyrolysis,* 91(1), 1–33.

Zobel N., Anca-Couce A., 2013, Slow pyrolysis of wood particles: characterization of volatiles by Laser-Induced Fluorescence, *Proc. Combust. Inst.*, 34, 2355–62.